Nuclear magnetic resonance and Mossbauer studies of rapidly quenched and heat-treated $Nd_4Fe_{77.5}B_{18.5}$ alloys



1992 J. Phys.: Condens. Matter 4 9147

(http://iopscience.iop.org/0953-8984/4/46/019)

J. Phys.: Condens. Matter 4 (1992) 9147–9152. Printed in the UK

# Nuclear magnetic resonance and Mössbauer studies of rapidly quenched and heat-treated $Nd_4Fe_{77.5}B_{18.5}$ alloys*

Mingxi Mao†, Chunli Yang†, Zhaohua Cheng†, Yide Zhang†, Baogen Shen‡, Linyuan Yang‡ and Fashen Li†

† Physics Department, Lanzhou University, Lanzhou 730000, People's Republic of China
‡ State Key Laboratory for Magnetism, Institute of Physics, Chinese Academy of Science, Beijing 100080, People's Republic of China

Received 23 April 1992, in final form 27 July 1992

**Abstract.** Using the Mössbauer effect and NMR, the phase compositions of rapidly quenched $Nd_4Fe_{77.5}B_{18.5}$ alloy under different heat treatment conditions were studied. It was shown that the sample which was annealed at 670 °C for a short time and has the optimal magnetic properties has a main BCT $Fe_3B$ phase containing Nd atoms and a small amount of $\alpha$-Fe (6%). It is concluded that the hard magnetic properties of crystallized melt-quenched Nd–Fe–B with a low Nd concentration do not originate from the presence of the hard magnetic $Nd_2Fe_{14}B$ phase but from the BCT $Fe_3B$ phase containing Nd atoms.

## 1. Introduction

Recently, many reports on the magnetic properties of crystallized melt-quenched Nd–Fe–B alloys with a low neodymium concentration have been given [1–4]. A coercivity of 3 kOe, a remanence magnetization of 12.5 kG and an energy product of 13 MG Oe were measured at room temperature for $Nd_4Fe_{77.5}B_{18.5}$ alloy annealed under an optimal heat treatment condition [5]. On comparison of the magnetic properties of crystallized melt-quenched Nd–Fe–B with a low Nd concentration (less than 5 at.%) with those of crystallized melt-quenched Nd–Fe–B with 12–16 at.% Nd, their $(BH)_{max}$-values are about the same and the remanence magnetization of the former is higher. Also it should be noted that the rare-earth concentration in the former is only about one third that in the latter. Until now, the origin of the hard magnetic properties of Nd–Fe–B alloy with a low Nd concentration has not been clarified and there is a lack of investigations on such materials by direct methods.

The Mössbauer effect and NMR are both important methods for researching the hyperfine interaction. Both methods can be employed to obtain information about the nearest-neighbour environment of the nuclei detected and some information on the phase composition which cannot be resolved by x-ray diffraction. Furthermore, NMR can measure the hyperfine field value $B_{hf}$ and its distribution more directly and more precisely while the Mössbauer effect can obtain a reliable relative intensity which is proportional to the on-site occupancies of the Fe atoms. In this work, we studied the phase composition of $Nd_4Fe_{77.5}B_{18.5}$ alloy under different treatment conditions using

* This project is supported by the National Natural Science Foundation of China.

0953-8984/92/469147+06$07.50  

the Mössbauer effect and NMR measurements, and the origin of the hard magnetic properties of such materials is discussed.

## 2. Experimental details

Alloys of $Nd_4Fe_{77.5}B_{18.5}$ were prepared by arc melting in an argon atmosphere of high purity. Amorphous ribbons about 1 mm wide and 20 $\mu$m thick were prepared using the melt-spinning technique at a speed of about 47 m $s^{-1}$. The heat treatment of as-quenched ribbons was performed in a steel tube evacuated to $2 \times 10^{-5}$ Torr at various temperatures.

The Mössbauer spectra were recorded at room temperature (RT) using a computer-controlled constant-acceleration Mössbauer spectrometer with a $^{57}Co(Pd)$ source. The zero-field NMR spectra of the $^{57}Fe$ and $^{11}B$ nuclei were measured at 8 K, a temperature attained using a circulation refrigerator, and at frequencies ranging from 20 to 60 MHz by a spin-echo NMR spectrometer which has a range from 20 to 360 MHz. The spin-echo amplitude was measured by a delay square signal with the same frequency as the spin-echo signal, and both of these were recorded and accumulated many times by a computer.

## 3. Results and discussion

### *3.1. Mössbauer results*

Figures 1(*a*), 1(*b*), 1(*c*), 1(*d*) and 1(*e*) show the Mössbauer spectra at RT of $Nd_4Fe_{77.5}B_{18.5}$ alloys under different heat treatment conditions, namely as-melted alloy, as-quenched amorphous ribbon, amorphous ribbon annealed at 670 °C for a short time, amorphous ribbon annealed at 839 °C for 60 min and amorphous ribbon annealed at 960 °C for 60 min, respectively. The phase compositions of the samples obtained using the fitted results are listed in table 1. From table 1 and figure 1, the following points are noted: as-melted alloy consists of $Fe_2B$, $Nd_2Fe_{14}B$, $\alpha$-Fe and a small amount of paramagnetic phase; the Mössbauer spectrum of amorphous ribbon is a typical amorphous broadened spectrum, the peak hyperfine field of which is 22.5 T and the average hyperfine field is 21.8 T; the sample annealed at 670 °C for a short time, which is the optimal treatment condition to obtain good hard magnetic properties, consists of a main BCT $Fe_3B$ phase and a small amount of $\alpha$-Fe (5%), but it should be noted that, in our Mössbauer spectrum for BCT $Fe_3B$, the relative intensity of the third subspectrum with the smallest hyperfine field corresponding to the Fe(III) 8g site is about 5% less than those of the other two; in the sample annealed at 839 °C, BCT $Fe_3B$ and $\alpha$-Fe coexist with a small amount of paramagnetic phase; the sample annealed at 960 °C is composed of $Fe_2B$, $Nd_2Fe_{14}B$, $\alpha$-Fe and a paramagnetic phase, which is similar to the case of the as-melted alloy.

### *3.2. NMR results*

Figure 2 shows the NMR spectra measured at 8 K for $Nd_4Fe_{77.5}B_{18.5}$ alloys under different heat treatment conditions as for figure 1. The results on the phase composition of different samples are also listed in table 1. In figure 2(*a*) and figure 2(*e*), the signal at 42.1 MHz resulting from $^{11}B$ in $Nd_2Fe_{14}B$ is so strong

**Table 1.** The results of the Mössbauer effect (at RT) and NMR (at 8 K). $T_1$ is $Nd_2Fe_{14}B$ and $T_2$ is the paramagnetic phase.

| $T_a$ | Crystalline phases | |
|---|---|---|
| (°C) | NMR | Mössbauer effect |
| As-melted alloy | $Fe_2B + T_1 + \alpha$-Fe | $Fe_2B + T_1 + \alpha$-Fe + $T_2$ (45.8%)(25.6%)(23.4%)(5.2%) |
| As-quenched ribbon | BCT $Fe_3B$ + orthorhombic $Fe_3B$ | Amorphous broadened spectrum |
| 670 | BCT $Fe_3B$ | BCT $Fe_3B + \alpha$-Fe (94.4%)(5.6%) |
| 839 | BCT $Fe_3B + \alpha$-Fe | BCT $Fe_3B + \alpha$-Fe + $T_2$ (60.9%)(30.9%)(8.2%) |
| 960 | $Fe_2B + T_1 + \alpha$-Fe | $Fe_2B + T_1 + \alpha$-Fe + $T_2$ (46.6%)(9.5%)(39.0%)(4.9%) |

that it overlaps all the Fe peaks between 41 and 47 MHz which originate from the $^{57}$Fe nuclei in the four Fe sites (4e, 4c, $16k_1$ and $8j_1$). The peak at 48.3 MHz comes from $^{57}$Fe in the $16k_2$ site. The signals at 52.0 and 53.0 MHz originating from $^{57}$Fe in the $8j_2$ site are too weak to be detected [6]. Therefore, the characteristic peaks of the $Nd_2Fe_{14}B$ phase in this kind of sample are the peaks at 42.1 and 48.3 MHz. For other phases, the peak at 40.5 MHz is from the $^{11}$B NMR signal of $Fe_2B$. The peaks at 36.3 and 34.7 MHz are from the $^{11}$B signals of orthorhombic $Fe_3B$ and BCT $Fe_3B$, respectively, and the peak at 46.7 MHz comes from $\alpha$-Fe [7–9].

From table 1 it is seen that, in many cases, both measurements gave the same results. Nevertheless, $\alpha$-Fe occurred in too small an amount to be found by NMR in the sample annealed at 670 °C and the paramagnetic phases were also not found by NMR because of the zero-field measurement. On the other hand, NMR results clarify that the type of short-range order for the as-quenched amorphous ribbon is BCT $Fe_3B$- and orthorhombic $Fe_3B$-like, which cannot be directly obtained from the Mössbauer measurement.

Table 1 shows the direct result of the influence of heat treatment on the phase composition. The well known 2:14:1 phase ($T_1$) formed in the as-melted alloy and the sample annealed at 960 °C; this implies that the $T_1$ phase is stable at high temperatures, but these two samples have almost no hard magnetic properties from our previous magnetic measurements [10]. In the other three samples, the metastable phase $Fe_3B$ is the main phase and there is no $T_1$ phase at all. In the as-quenched amorphous ribbon, BCT $Fe_3B$ and orthorhombic $Fe_3B$ are the main phases according to the results of NMR measurements. In the samples annealed at 670 and 839 °C, only BCT $Fe_3B$ constitutes the main phase. Another interesting point is that, in the sample annealed under the optimal condition of 670 °C for a short time, the $^{11}$B NMR peak from the main BCT $Fe_3B$ phase broadens on the high-frequency side, and this can be clearly seen in figure 2(*c*). However, in the sample annealed at a higher temperature of 839 °C, this peak distortion disappears (figure 2(*d*)). The peak distortion of BCT $Fe_3B$ is not related to orthorhombic $Fe_3B$, the $^{11}$B NMR resonance of which occurs at 36.3 MHz, because firstly orthorhombic $Fe_3B$ was not found by the Mössbauer effect and secondly the upper limit (39.0 MHz) of the broadening on the high-frequency side of this peak distortion is higher than that (37.3 MHz) of ordinary orthorhombic $Fe_3B$ in crystallized Fe–B-based amorphous alloys [8, 9].

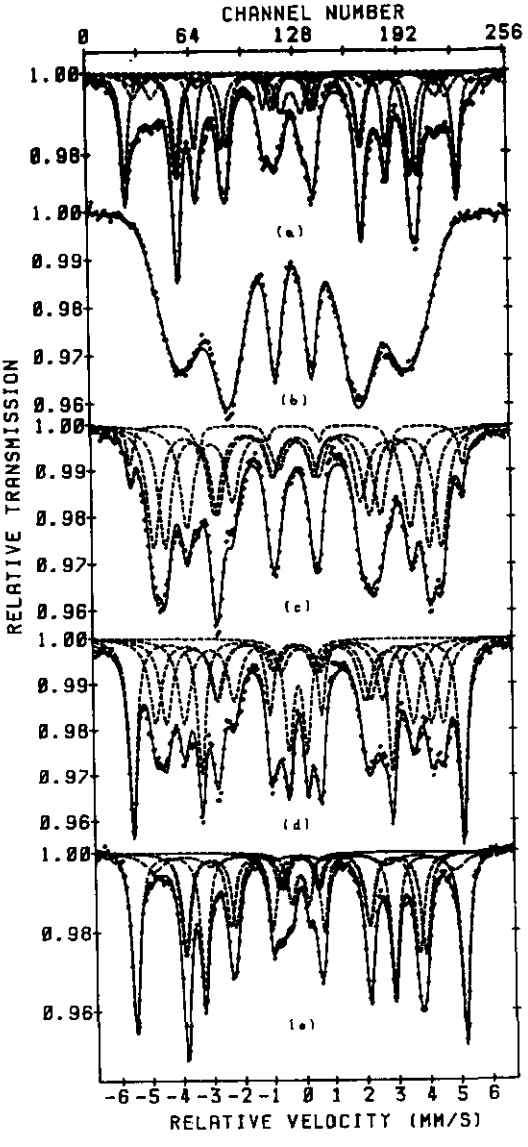


**Figure 1.** Mössbauer spectra of $Nd_4Fe_{77.5}B_{18.5}$ alloys under different heat treatment conditions at room temperature: (*a*) as-melted alloy; (*b*) as-quenched amorphous ribbon; (*c*) amorphous ribbon annealed at 670 °C for a short time; (*d*) amorphous ribbon annealed at 839 °C for 60 min; (*e*) amorphous ribbon annealed at 960 °C for 60 min.

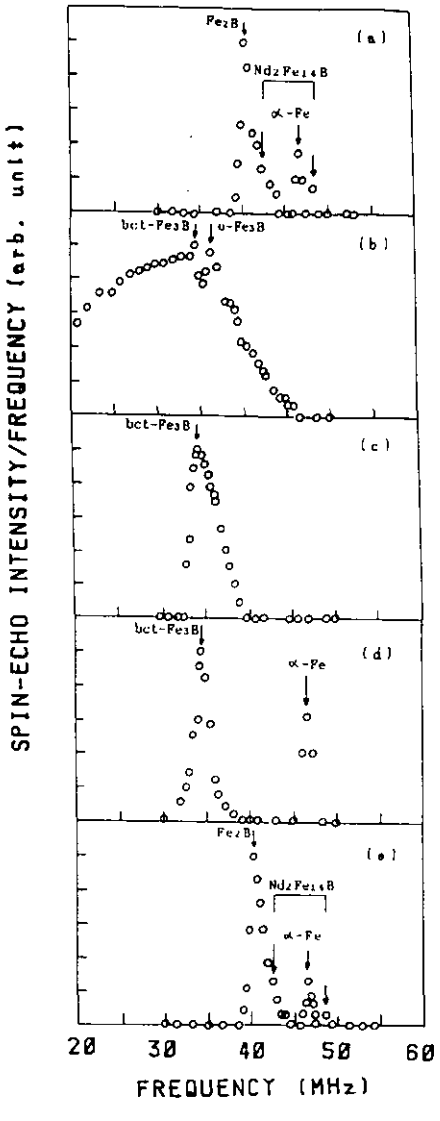


**Figure 2.** NMR spectra of $Nd_4Fe_{77.5}B_{18.5}$ alloys under different heat treatment conditions at 8 K: (*a*) as-melted alloy; (*b*) as-quenched amorphous ribbon; (*c*) amorphous ribbon annealed at 670 °C for a short time; (*d*) amorphous ribbon annealed at 839 °C for 60 min; (*e*) amorphous ribbon annealed at 960 °C for 60 min. The peaks are at 34.7 MHz for $^{11}B$ in BCT $Fe_3B$, at 36.3 MHz for $^{11}B$ in orthorhombic $Fe_3B$, at 40.5 MHz for $^{11}B$ in $Fe_2B$, at 42.1 MHz for $^{11}B$ in $Nd_2Fe_{14}B$, at 48.3 MHz for $^{57}Fe$ in the $16k_2$ site of $Nd_2Fe_{14}B$ and at 46.7 MHz for $^{57}Fe$ in $\alpha$-Fe.

### *3.3. Discussion*

The NMR and Mössbauer results clearly demonstrate that only BCT $Fe_3B$ and a small

**Table 2.** Mössbauer fitting parameters of $Nd_4Fe_{77.5}B_{18.5}$ annealed at 670 °C for 2 min.

| Component | Content (%) | Linewidth (mm $s^{-1}$) | IS[a] (mm $s^{-1}$) | QS (mm $s^{-1}$) | HF (T) |
|---|---|---|---|---|---|
| α-Fe | 5.6 | 0.26 | 0.00 | 0.02 | 33.3 |
| BCT $Fe_3B$ (I) | 33.2 | 0.51 | 0.06 | −0.01 | 28.8 |
| BCT $Fe_3B$ (II) | 33.2 | 0.51 | −0.01 | 0.04 | 26.4 |
| BCT $Fe_3B$ (III) | 28.0 | 0.51 | 0.08 | 0.02 | 22.4 |

[a] The isomer shift here is relative to α-Fe.

amount of α-Fe exist in the sample with the best hard magnetic properties. It is well known that both NMR and the Mössbauer effect can give local information and detect the magnetically hard and randomized phase without any external field; this is because a very large hyperfine field exists in magnetically ordered materials. For the small-grain particles, whose sizes are smaller than the size of the single domain, their NMR signals are weaker than those of multi-domain particles because the former's domain wall disappears and the enhancement factor of a domain is smaller than that of a domain wall [9]. It is possible that the signals originating from the domain are too weak to be detected by NMR, but Mössbauer measurements are not influenced by the difference between a domain and a domain wall. On the other hand, we should note that there is a much lower possibility that the signal of the $Nd_2Fe_{14}B$ phase overlaps that of the BCT $Fe_3B$. For NMR, the difference between the hyperfine fields at B- and Fe-site nuclei in BCT $Fe_3B$ and in $Nd_2Fe_{14}B$ is very large. For the Mössbauer effect, a subspectrum with an average hyperfine field of 30.1 T for $Nd_2Fe_{14}B$ does not appear between the hyperfine field of 33.1 T for α-Fe and the hyperfine field of 28.8 T for the first subspectrum of BCT $Fe_3B$ and in figure 1(*c*) the sixth peak of the $8j_2$ site in $Nd_2Fe_{14}B$, which is the main peak of $Nd_2Fe_{14}B$, cannot be found. When some $Nd_2Fe_{14}B$ appears, both NMR and the Mössbauer effect demonstrate its existence, e.g. in the sample annealed at 960 °C. So, even though some $Nd_2Fe_{14}B$ exists in the sample annealed at 670 °C, its concentration must be too low to be detected, and such a small amount of $Nd_2Fe_{14}B$ cannot generate a high coercivity. Meanwhile, according to our results, when some $Nd_2Fe_{14}B$ phase appears, e.g. for the sample annealed at 960 °C and the as-melted alloy, its hard magnetic properties are very poor. So, it can be concluded that the origin of the hard magnetic properties in crystallized melt-quenched Nd–Fe–B with a low Nd concentration is not related to the 2:14:1 hard magnetic phase.

Now, we consider the interesting questions of where the Nd atoms have gone and what the origin of hard magnetic properties in this kind of material is. From figure 1(*c*) and figure 2(*c*), we can see that the $^{57}Fe$ Mössbauer and $^{11}B$ NMR spectra of BCT $Fe_3B$ in the sample annealed at 670 °C for a short time are different from those of pure BCT $Fe_3B$. The $^{57}Fe$ Mössbauer spectrum indicates the relative intensity of the third subspectrum corresponding to the Fe(III) 8g site of BCT $Fe_3B$ is about 5% less than those of the other two subspectra, and this value of 5% is approximately equal to the Nd concentration. The $^{11}B$ NMR spectrum broadens on the high-frequency side, which shows that there are some fluctuations in the nearest-neighbour environment of B atoms. These results indicate that the Nd atoms enter the BCT $Fe_3B$ phase and substitute for the Fe atoms in the Fe(III) 8g sites of BCT $Fe_3B$.

It is well known that BCT $Fe_3B$ is a good soft magnetic phase and $Nd_2Fe_{14}B$ is a good hard magnetic phase. In these two phase structures, each B atom is always

located in the centre of a trigonal prism formed by the six nearest Fe atoms, but the scales of these prisms and, consequently, the Fe–B and Fe–Fe distances are different [9]. In the BCT $Fe_3B$ structure the B atom is located in the centre of the trigonal prism formed by the six nearest Fe atoms; three other Fe atoms are situated at a slightly longer distance and bonded to each B atom through a rectangular prism face. If these three Fe atoms are replaced by three Nd atoms, the local environment will be similar to that of $Nd_2Fe_{14}B$ [11]. Therefore, when Nd atoms enter BCT $Fe_3B$, it is reasonable to suppose that BCT $Fe_3B$ containing Nd atoms may have better hard magnetic properties owing to the large anisotropy of Nd ions. For the sample annealed at 839 °C, the distortion of the $^{11}B$ NMR peak of BCT $Fe_3B$ disappears (figure 2(*d*)), the three Mössbauer subspectra of BCT $Fe_3B$ have the same relative intensities and the Nd atoms from BCT $Fe_3B$ form a paramagnetic phase with Fe and B atoms (figure 1(*d*)). As a result, the hard magnetic properties become much worse. So, it is concluded that BCT $Fe_3B$ containing Nd atoms might be responsible for the good hard magnetic properties in crystallized melt-quenched Nd–Fe–B with a low Nd concentration.

## 4. Summary

(1) From the results of the Mössbauer effect and NMR measurements, the sample with the best hard magnetic properties consists of a main BCT $Fe_3B$ phase containing Nd atoms and a small amount of $\alpha$-Fe without the existence of the $Nd_2Fe_{14}B$ phase.

(2) When some $Nd_2Fe_{14}B$ appears, e.g. for the sample annealed at 960 °C and the as-melted alloy, the hard magnetic properties disappear fully.

(3) The hard magnetic properties in crystallized melt-quenched Nd–Fe–B with a low Nd concentration do not originate from the presence of the hard magnetic 2:14:1 phase.

(4) The origin of the hard magnetic properties in crystallized melt-quenched Nd–Fe–B with a low Nd concentration is related to the fact that Nd atoms substitute in the Fe(III) 8g sites of the BCT $Fe_3B$ lattice. Further research is in progress.

## References

[1] Coehoorn R, de Mooij D B and de Waard C 1989 *J. Magn. Magn. Mater.* **80** 101
[2] Gu B X, Shen B G, Methfessel S and Zhai H R 1989 *Solid State Commun.* **70** 933
[3] Shen B G, Ding J, Gu B X, Zhang Z Y, Homburg H, Zhao J G and Methfessel S 1990 *J. Magn. Magn. Mater.* **92** 53
[4] Yang L Y, Shen B G, Zhang J X, Wo F, Ning T S, Zhao J G, Guo H Q and Zhan W S 1990 *J. Less-Common Met.* **166** 189
[5] Shen B G, Zhang J X, Yang L Y, Wo F, Ning T S, Ji S Q, Zhao J G, Guo H Q and Zhan W S 1990 *J. Magn. Magn. Mater.* **89** 195
[6] Zhang Y D, Budnick J I, Yang D P, Potenziani II E, Pedziwiatr A T, Wallace W E and Sagawa M 1989 *J. Magn. Magn. Mater.* **79** 136
[7] Zhang Y D, Budnick J I, Ford J C, Hines W A and Sanchez F H 1987 *J. Appl. Phys.* **61** 3231
[8] Mao M X, Ge S H, Cheng Z H, Cheng G L, Zhang C L and Zhang Y D 1993 *J. Appl. Phys.* to appear
[9] Zhang Y D, Budnick J I, Ford J C and Hines W A 1991 *J. Magn. Magn. Mater.* **100** 13
[10] Shen B G, Zhang J X, Yang J Y, Wo F, Ning T S, Zhao J G, Guo H Q and Zhan W S 1991 *J. Less-Common Met.* **167** 339
[11] Herbst J F, Croat J J, Pinkerton F D and Yelon M B 1984 *Phys. Rev.* B **29** 4176